JACS
JOURNAL OF THE AMERICAN CHEMICAL SOCIETY

Article

pubs.acs.org/JACS

Self-Assembled Near-Infrared Dye Nanoparticles as a Selective Protein Sensor by Activation of a Dormant Fluorophore

Palapuravan Anees,[†,‡] Sivaramapanicker Sreejith,[†] and Ayyappanpillai Ajayaghosh*[,†,‡]

[†]Chemical Sciences and Technology Division and [‡]Academy of Scientific and Innovative Research (AcSIR), CSIR-National Institute for Interdisciplinary Science and Technology (CSIR-NIIST), Trivandrum 695019, India

Supporting Information

ABSTRACT: Design of selective sensors for a specific analyte in blood serum, which contains a large number of proteins, small molecules, and ions, is important in clinical diagnostics. While metal and polymeric nanoparticle conjugates have been used as sensors, small molecular assemblies have rarely been exploited for the selective sensing of a protein in blood serum. Herein we demonstrate how a nonspecific small molecular fluorescent dye can be empowered to form a selective protein sensor as illustrated with a thiol-sensitive near-IR squaraine (**Sq**) dye (λ_{abs}= 670 nm, λ_{em}= 700 nm). The dye self-assembles to form nonfluorescent nanoparticles (D_h = 200 nm) which selectively respond to human serum albumin (HSA) in the presence of other thiol-containing molecules and proteins by triggering a green fluorescence. This selective response of the dye nanoparticles allowed detection and quantification of HSA in blood serum with a sensitivity limit of 3 nM. Notably, the **Sq** dye in solution state is nonselective and responds to any thiol-containing proteins and small molecules. The sensing mechanism involves HSA specific controlled disassembly of the **Sq** nanoparticles to the molecular dye by a noncovalent binding process and its subsequent reaction with the thiol moiety of the protein, triggering the green emission of a dormant fluorophore present in the dye. This study demonstrates the power of a self-assembled small molecular fluorophore for protein sensing and is a simple chemical tool for the clinical diagnosis of blood serum.

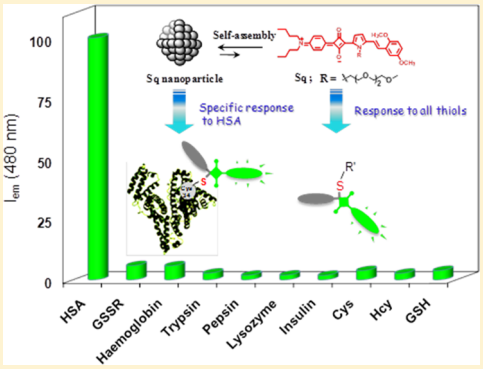

INTRODUCTION

Over the years, molecular self-assembly has matured into a powerful tool for the construction of soft functional materials having wide ranging applications in materials science and biology.[1] Many of these dimensionally tunable soft architectures are enormously powerful when compared to their individual molecular building blocks in terms of physical or chemical properties.[2] While metal and polymeric nanoparticles provide versatile scaffolds as sensors for proteins, use of small molecule-based nanoparticles has not been much exploited in protein sensing applications. Herein we demonstrate that a thiol-sensitive near-infrared (NIR) dye becomes a powerful tool for the specific sensing of serum albumin proteins (SAP) in the presence of other competing thiol-containing proteins and small molecules, only when the dye self-assembles to form nanoparticles, whereas in the isotropic solution state, the dye responds to all thiol-containing molecules, losing the selectivity.

Protein sensing and imaging are important in clinical diagnosis to detect protein biomarkers and in biology to explore cellular processes.[3] Previously, several strategies have been reported for protein sensing.[4−8] These strategies are mainly based on fluorophores, which lack selectivity in many cases and have the disadvantage of small-to-moderate fluorescence response due to high background noise signals. Recently, Thayumanavan and co-workers have extensively studied the use of polymer nanoparticle disassembly approach for protein sensing.[9,10] The disassembly driven turn-on fluorescence approach reported by Hamachi and co-workers makes use of a ligand-protein affinity labeling which requires integration of a fluorophore with a suitable ligand through elaborate synthetic procedures.[11,12] Alternatively, Rotello and co-workers have reported array of green fluorescent protein (GFP) and gold nanoparticle conjugates for multiple protein analysis in blood serum.[13] Nevertheless, selective detection of a target analyte among thousands of others present in a biofluid using a small molecular fluorophore-based sensor continues to be a challenge to chemists. While metal nanoparticles, polymers and affinity ligand-based sensors have their merits and demerits, the small molecule-based sensor described here is the simplest and easy to operate.

Thiol-containing proteins are important in biological functions and are present in high concentrations in blood serum. Among different thiol-containing proteins in blood, human serum albumin (HSA) plays a key role in maintaining human health.[14,15] Variation in HSA concentration indicates liver and kidney diseases or malnutrition owing to a low protein diet. Contrarily, severe or chronic dehydration has been related to an excess of albumin. Detection of HSA in blood serum with a fluorescent molecular probe is often interfered by the

Received: April 17, 2014
Published: September 8, 2014

dx.doi.org/10.1021/ja503850b | J. Am. Chem. Soc. 2014, 136, 13233−13239

nonspecific covalent interaction with competing proteins. Moreover, blood serum has a large number of thiol-containing molecules present in small quantities, and hence thiol responsive probes cannot be used for selective HSA sensing in biofluids. This is due to the high affinity of thiol group with the reactive site of the molecular sensors.[16,17] Therefore, a selective, sensitive, and simple fluorescent sensor with controlled reactivity is required for the diagnosis of HSA in blood serum. Squaraines are an important class of dyes which are extensively used as probes for the detection of cations,[18,19] neutral molecules,[20] proteins,[21] and for imaging of cells.[22−24] However, squaraine dyes in general have the tendency to form aggregates under aqueous conditions which is a drawback for their use due to the strong quenching of the emission.[25] In this work, we explore this otherwise unfavorable property and prove that the aggregation of a fluorescent squaraine dye to nonfluorescent nanoparticles can be turned around as an opportunity to the selective sensing of SAP in the presence of other competing biomolecules.

The underlying mechanism of our sensing strategy involves the noncovalent interaction of the protein with the nanoparticles and the consequent controlled disassembly driven selective covalent interaction of free cysteine residue in SAP with the dye molecule (Figure 1). Initially, the fluorescent **Sq**

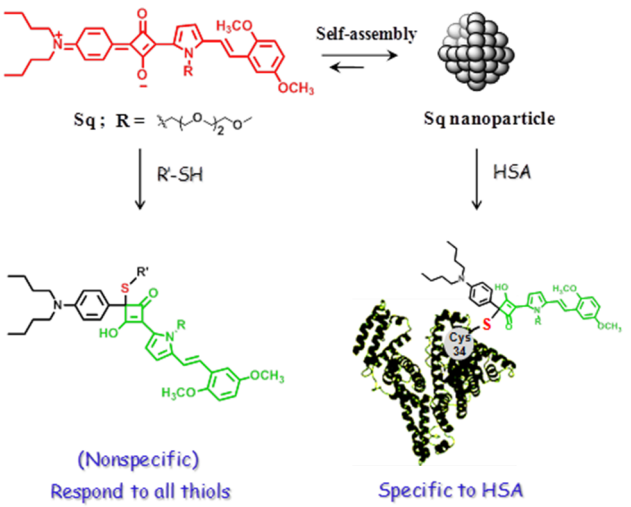

Figure 1. A schematic representation of the **Sq** dye nanoparticle for the specific sensing of SAP. The NIR emitting squaraine dye, **Sq** in the monomeric state (30% acetonitrile/phosphate buffer pH 8.0) interact nonspecifically to all thiol-containing proteins and small molecules, whereas the nonemissive **Sq** nanoparticles (in phosphate buffer, pH 8.0) interact specifically with SAP to trigger a green emission at 480 nm.

dye undergoes aggregation and self-assembly in aqueous medium to form nonfluorescent spherical nanoparticles in which the dye remains chemically dormant. Therefore, the **Sq** nanoparticles are found nonreactive to small molecular thiols. However, addition of bovine serum albumin (BSA) or HSA induces the disassembly of the dye nanoparticles that facilitates encapsulation of the dye in the hydrophobic pockets of the protein. This process reactivates the dye and triggers its reaction with the cysteine residue at the 34th position of the protein. The chemistry involves a base catalyzed nucleophilic addition of the thiol moiety to the cyclobutene double bond of the **Sq** dye at a pH of 7.0−8.0. This addition reaction results in the breakage of conjugation of the dye to generate a new chromophore in situ that activates a strong green fluorescent signal. On the other hand, a homogeneous solution of **Sq** dye responds to any thiol-containing molecules, triggering fluorescent signals without any selectivity. This remarkable selectivity of the **Sq** nanoparticles when compared to the molecular dye facilitates the use of the former as a selective sensor for the detection of albumin content in human blood serum in the presence of other competing biomolecules and proteins.

RESULTS AND DISCUSSION

The squaraine dye **Sq** was synthesized by the reaction of the strongly fluorescent styrylpyrrole with the semisquaraine derivative of *N*,*N*-dibutyl aniline in the presence of tributylorthoformate (TBOF) and isopropanol in a 40% yield. The dye was purified by column chromatography (silica gel, 2% methanol-chloroform) and characterized by ^{1}H and ^{13}C NMR and mass spectral analyses (Supporting Information). A solution of **Sq** in acetonitrile (2 μM) showed an absorption maximum at 670 nm and an emission maximum at 700 nm (Φ_F = 0.083, determined using indicarbocyanine dye in methanol as standard). Addition of phosphate buffer (pH 8.0) into an acetonitrile solution of the dye resulted in the broadening of the absorption spectrum in the 550−850 nm range and the gradual quenching of the emission at 700 nm (Figures 2a and

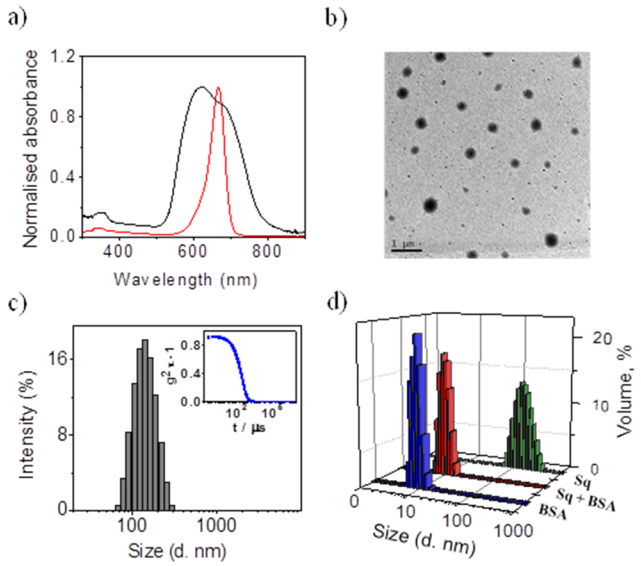

Figure 2. (a) UV−vis absorption spectra of **Sq** in acetonitrile (red line) and 25 mM phosphate buffer (black line). (b) TEM and (c) DLS analyses of **Sq** (6 μM) spherical assemblies obtained from 25 mM phosphate buffer at a pH of 8.0. (d) DLS analysis of **Sq** (6 μM) in the presence and absence of BSA protein (12 μM). DLS data of BSA protein alone (6 μM) are also shown.

S1). This change in the absorption spectrum indicates the aggregation of the dye which was further confirmed by temperature-dependent UV−vis absorption and emission spectroscopic studies in 15% acetonitrile/phosphate buffer (pH 8.0) mixture (Figure S2). When the solution temperature was increased from 25 to 70 °C, a significant increase in the absorption intensity at 670 nm was observed, indicating the disassembly of the aggregates to the monomeric dye.

dx.doi.org/10.1021/ja503850b | J. Am. Chem. Soc. 2014, 136, 13233−13239

Atomic force microscopy (AFM) and transmission electron microscopy (TEM) revealed the formation of spherical particles of the dye with diameters ranging from 100 to 300 nm (Figure S3 and Figure 2b). The nanoparticle formation was further confirmed by dynamic light scattering (DLS) experiments of a buffer solution containing **Sq** (6 μM) which showed particles with a mean diameter of 200 nm (Figure 2c). The dynamic correlation data show the characteristic of spherical particles (Figure 2c, inset). In an attempt to encapsulate and stabilize the **Sq** nanoparticles within a protein matrix, we added bovine serum albumin (BSA) in a phosphate buffer (6 μM) at a pH 8.0. Surprisingly, DLS analysis after the addition of BSA showed the disappearance of the peak at 200 nm corresponding to the **Sq** nanoparticles with the appearance of a new band at 10 nm which corresponds to the size of the globular protein (Figure 2d).[26] This observation reveals that the BSA protein interacts with the **Sq** nanoparticles, leading to a gradual disassembly of the latter. Similar observation was found when HSA was added to **Sq** nanoparticles. For a deeper understanding, the response of **Sq** nanoparticles was investigated with the addition of a large number of other proteins which did not show any variation in the DLS data indicating that proteins other than BSA and HSA do not interact with the dye nanoparticles (Figure S4).

In the light of the above findings, we studied the changes in the absorption and emission spectral properties of the **Sq** nanoparticles with SAP. For this purpose, we used BSA instead of HSA since the former is easily available and cheaper but structurally similar to the latter. Addition of BSA to **Sq** nanoparticles (6 μM) in phosphate buffer at a pH of 8.0 resulted in the decrease of the broad absorption band 670 nm with the formation of a new band at 380 nm (Figure 3a). The dye nanoparticles initially had no emission at the 480 nm region when excited at 380 nm, however addition of BSA resulted in the formation of a band at 480 nm (Figure 3b). The light-blue solution of **Sq** nanoparticles became pale yellow (Figure 3a, inset) in color with the appearance of a green emission upon the addition of BSA (Figure 3b, inset) in the phosphate buffer at a pH of 8.0. Similar behavior was observed with the addition of HSA (Figure S5). The fluorescence intensity increased linearly with the increase in concentration of the protein between 0−100 nM indicating a broad detection range. From the fluorescence intensity variation (above 5% of the initial fluorophore emission), the lower detection level of BSA and HSA was found as 3 nM (Figure S6). Below this concentration, no detectable fluorescence variation could be noticed.

The selectivity of our probe toward SAP was established in the presence of other thiol-containing proteins such as glutathione reductase (GSSR), hemoglobin, bromelain, and small thiol-containing molecules such as cysteine (Cys), homocysteine (Hcy), glutathione (GSH), mercaptoethanol (ME), dithiothreitol (DTT), thioglycolic acid (TGA), and cysteamine. Excess (10 equiv) of these thiol-containing molecules could not change the fluorescence intensity at the 480 nm region (Figure 4a,b) indicating that thiol group in these molecules are nonresponsive to the **Sq** nanoparticles. The selectivity could be visually observed by adding different thiol-containing proteins and small molecules in a microwell plate filled with the **Sq** nanoparticle solution. Under UV illumination, green fluorescence was observed only for wells containing BSA and HSA (Figure 4a inset). This observation reveals the enhanced selectivity of **Sq** nanoparticles toward the free

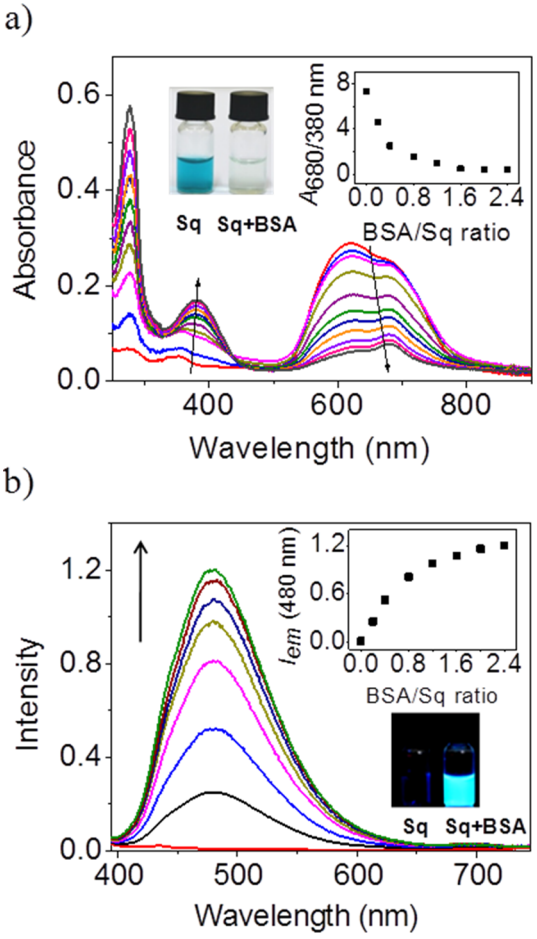

Figure 3. (a) UV−vis absorption and (b) emission spectral changes of **Sq** nanoparticles upon addition of BSA protein (0−14 μM) (λ_{exc} @ 380 nm). Arrows indicate the relative change in absorption and emission with increase in concentration of BSA protein. Plots of the absorption (top) emission (bottom) intensity vs BSA concentration and photographs of **Sq** nanoparticles before and after addition of BSA protein under UV illumination (365 nm) are shown in the inset.

cysteine residue in SAP in the presence of similar competing functional groups.

In order to establish the role of **Sq** nanoparticles in the selective sensing of SAP, we investigated the response of the **Sq** dye in its monomeric form with various thiol-containing molecules. For this purpose, the **Sq** dye solution in 30% acetonitrile/phosphate buffer at pH 8.0 is prepared. Under this condition, the dye exists in the monomeric state, which is clear from the absorption maximum at 670 nm and emission maximum at 700 nm (Figure S1). Upon addition of GSH, the absorbance at 670 nm was decreased with the concomitant formation of a new band at 380 nm (Figure 5a). When excited at 380 nm followed by addition of GSH, the emission spectrum of **Sq** solution exhibited a new band at 510 nm with a green fluorescence, whereas the NIR emission intensity at 700 nm of the **Sq** dye was decreased (Figures 5b and S7).

We further studied the effect of different thiol-containing molecules such as Cys, Hcy, ME, DTT, TGA, and cysteamine with **Sq** solution. These thiols exhibited fluorescence enhancement at 510 nm with the concomitant decrease of the intensity at 700 nm (Figure 5c), indicating that, though **Sq** in their self-assembled state is specific to cysteine residue of the SAP, in the monomeric state, **Sq** does not show selectivity toward any

dx.doi.org/10.1021/ja503850b | J. Am. Chem. Soc. 2014, 136, 13233−13239

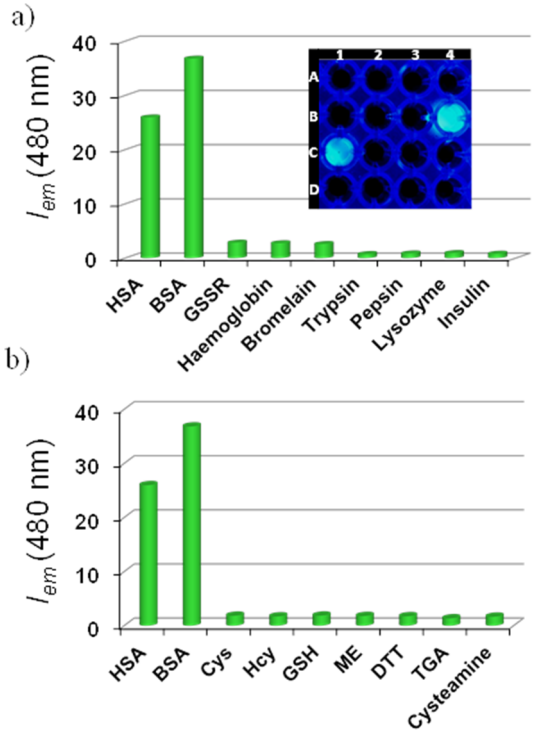

Figure 4. (a and b) Fluorescence response of **Sq** nanoparticles at 480 nm (λ_{exc} @ 380 nm) monitored against 1 equiv of HSA and BSA and 10 equiv of different proteins and small molecules. Inset in (a) shows photograph of various proteins and small molecules in a microwell plate containing **Sq** nanoparticles under UV illumination (365 nm). Well A1 (GSSR), A2 (hemoglobin), A3 (bromelaine), A4 (trypsin), B1 (pepsin), B2 (lysozyme), B3 (insulin), B4 (BSA), C1 (HSA), C2 (Cys), C3 (Hcy), C4 (GSH), D1 (ME), D2 (DTT), D3 (TGA), D4 (cysteamine). All experiments were performed using 6 μM **Sq** nanoparticle solution in 25 mM phosphate buffer at pH 8.0.

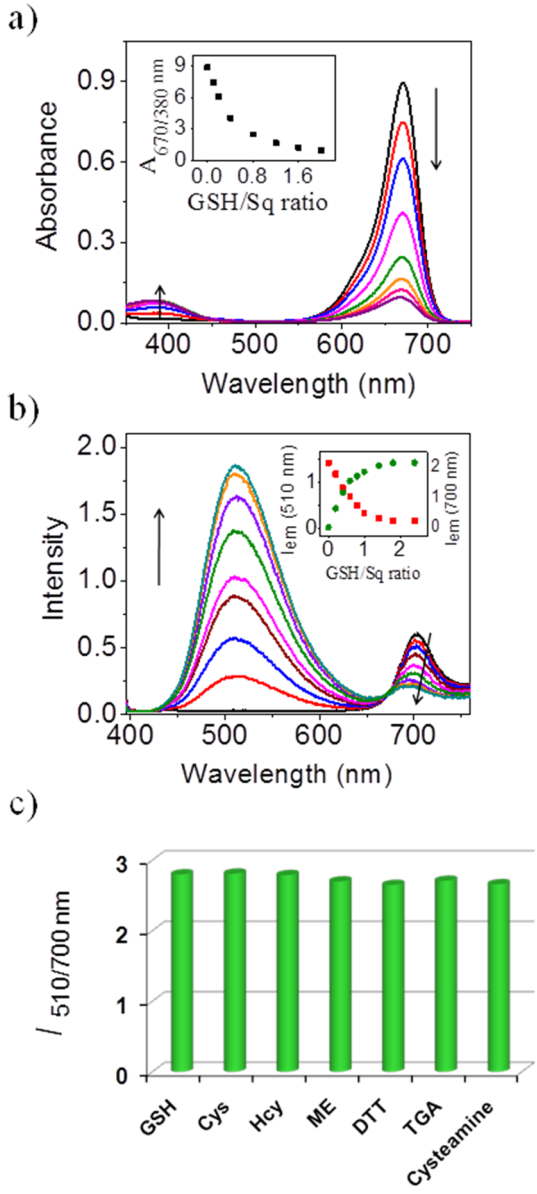

Figure 5. (a) UV−vis absorption and (b) fluorescence responses of **Sq** (2 μM) upon addition of GSH (0−4 μM) (λ_{exc} @ 380 nm). (c) Fluorescence response of **Sq** (2 μM) at 510 and 700 nm (λ_{exc} @ 380 nm) with different thiol-containing molecules (4 μM). These experiments were performed in 30% acetonitrile/25 mM phosphate buffer at pH 8.0.

specific thiols. Moreover, the fluorescence intensity of **Sq** changes only with thiol-containing molecules and not with other nonthiolated molecules (Figure S8). In order to confirm the addition of thiol with **Sq** dye, we prepared a thiol adduct of **Sq** with hexanethiol which displayed a peak at m/z 777.8 corresponding to the **Sq**-hexanethiol adduct (Figure S9).

A practical use of the **Sq** nanoparticles is established by the estimation of HSA content in blood serum. Addition of aliquots of the blood serum samples (10, 20, 30, and 40 μL) to **Sq** nanoparticles (6 μM, in phosphate buffer pH 8.0) showed an enhancement of the fluorescence intensity at 480 nm (Figure 6a). The HSA contents were estimated from the fluorescence intensity values using a calibration graph (Figure S10). A comparative plot of the concentrations of HSA in different blood samples using the **Sq** nanoparticles and those obtained for the same blood samples by the standard clinical test (obtained independently from a clinical laboratory) is shown in Figure 6b. The values obtained using our protocol were slightly lower than those obtained from the standard clinical laboratory analysis. The relative lower values of our method further reveal that the free thiols present in blood serum in small quantities do not interfere with the analysis of HSA as also independently established by the detection of HSA in the presence of equivalent amount of added thiols (Figure S11). Since, it is known that the clinical method sometimes may overestimate the albumin content, the **Sq** nanoparticle-based protocol described in this work can be used when a more accurate estimation is needed (accurate up to the third decimal).[27]

From the above experimental observations, we hypothesized that the protein selectivity could be due to the characteristic tertiary structure of the SAP which may be responsible for the disassembly of the **Sq** nanoparticles and the subsequent binding with the protein. In order to prove this hypothesis, we reduced the disulfide bonds that maintain the tertiary structure in SAP using DTT reagent. The reduced proteins, despite of having more numbers of thiol groups, showed relatively weak fluorescence response to **Sq** nanoparticles when compared to that of the native proteins (Figure 7a). DLS analysis of the **Sq** nanoparticles in the presence of the denatured proteins at pH 8.0 did not show any change in the size distribution corresponding to the **Sq** nanoparticles (Figure S12). This

dx.doi.org/10.1021/ja503850b | J. Am. Chem. Soc. 2014, 136, 13233−13239

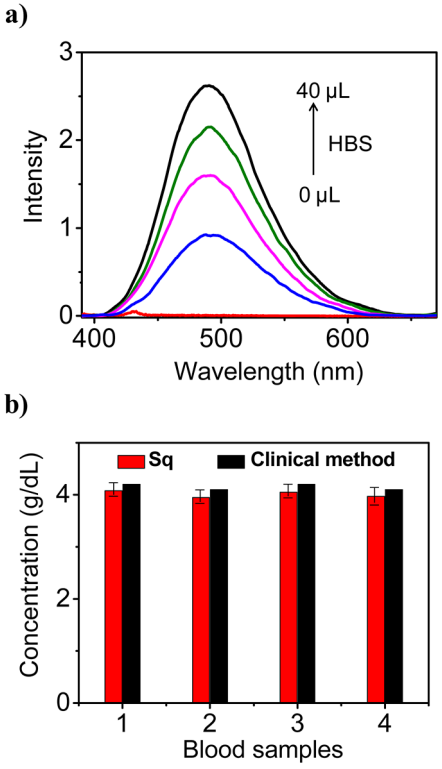

Figure 6. (a) Emission intensity change of **Sq** nanoparticles (6 μM) in 25 mM phosphate buffer, pH 8.0 at 480 nm (λ_{exc} @ 380 nm) upon addition of aliquots (0, 10, 20, 30, and 40 μL) of human blood serum (HBS). (b) Validation of data obtained using **Sq** nanoparticles with those obtained independently from a clinical laboratory using the standard procedure.[27]

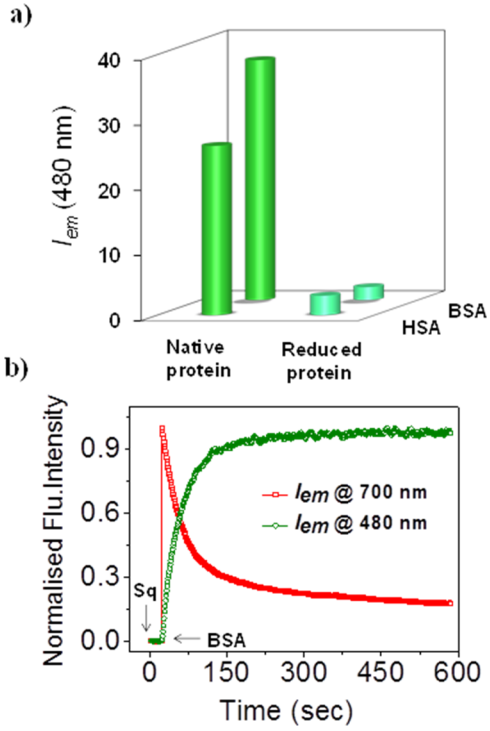

Figure 7. (a) Fluorescence response of **Sq** at 480 nm (λ_{exc} @ 380 nm) upon addition of 1 equiv of native and denatured BSA and HSA proteins. (b) Time-dependent fluorescence response of 1:10 **Sq**-BSA at 480 (λ_{exc} @ 380 nm, green) and 700 nm (λ_{exc} @ 380 nm, red). All experiments were performed using 6 μM **Sq** in 25 mM phosphate buffer at pH 8.0.

observation indicates that the denaturing of the tertiary structure of the protein does not facilitate the disassembly of the **Sq** nanoparticles, thus preventing the interaction of the thiol moiety with the dye. The SAP-induced disassembly of **Sq** nanoparticles may be driven by the strong affinity for the binding of the **Sq** dye at the hydrophobic sites of the protein.[28] Squaraine dyes are known to interact with SAP selectively by a combination of hydrophobic, hydrogen bonding, and electrostatic interactions.[21]

If the addition of SAP induces the disassembly of the **Sq** nanoparticles and its subsequent noncovalent binding within the hydrophobic pocket, the native NIR fluorescence of the molecular dye should be observed. This noncovalent interaction pathway that occurs before the covalent modification of the protein is confirmed by a time-dependent fluorescence monitoring of the **Sq**-BSA complex at 700 nm (λ_{exc} @ 640 nm) (Figure 7b). Addition of 10 equiv of BSA protein into the **Sq** nanoparticles (6 μM, phosphate buffer, pH 8.0) immediately enhanced the fluorescence intensity at 700 nm. With time, the fluorescence intensity at 700 nm decreased, and the fluorescence intensity at 480 nm increased indicating the covalent addition of the SAP thiol moiety to the dye. This study confirms the initial complexation of the dye with the protein before it undergoes covalent thiol addition which is responsible for the selective sensing of SAP even in the presence of free thiols.

CONCLUSIONS

We have demonstrated the versatility of an organic dye nanoparticle for the sensing of SAP in a pool of other biomolecules. **Sq** dye in its native molecular form is reactive to a variety of thiol-containing molecules. However, when the dye self-assembles to form nanoparticles, only SAP could selectively interact with the dye thereby opening the access for a thiol attack. Thus, the dormant fluorescence moiety present in the **Sq** dye gets activated latently, allowing the specific sensing of SAP by "turn-on" green fluorescence. The fact that this selective covalent modification of SAP is achieved only with the self-assembled system and not with the monomeric dye does make the **Sq** nanoparticles a selective supramolecular fluorescent sensor. The enhanced selectivity of the **Sq** nanoparticles allowed us to use them for the quantitative estimation of HSA in human blood samples. The described self-assembly approach using a small organic NIR dye having a dormant fluorophore, which is latently activatable through a nucleophilic attack is a model example for empowering a small molecular fluorophore to a reaction-specific nanosensor by self-assembly. This work is expected to encourage scientists to design similar systems for sensing and imaging of biorelevant molecules by exploring the unlimited potential of molecular self-assemblies.

EXPERIMENTAL SECTION

Materials and Reagents. Unless otherwise stated, all materials and reagents were purchased from commercial suppliers. The solvents were purified and dried by standard methods prior to use. Human serum albumin (HSA), bovine serum albumin (BSA), glutathione reductase (GSSR), hemoglobin, bromelain, trypsin, pepsin, lysozyme,

dx.doi.org/10.1021/ja503850b | J. Am. Chem. Soc. 2014, 136, 13233−13239

and other amino acids were purchased from Sigma-Aldrich. All other reagents were of analytical grade and were used without further purification. Reactions were performed under inert atmosphere of nitrogen unless specified otherwise. The pyrrole derivative **7** and the semisquaraine derivative **10** were prepared as per literature reports.[29,30]

Preparation of Sq Nanoparticles. A stock solution of **Sq** (1.2×10^{-3} M) was prepared from acetonitrile. Fifteen μL of this solution was injected into phosphate buffer (3 mL) maintained at pH 8.0, and the solution (6×10^{-6} M) was kept under room temperature. The green color of the stock solution turned blue indicating aggregation of the dye. Nanoparticle formation was confirmed by AFM and TEM analyses of the solution by drop casting on freshly cleaved mica surface or carbon-coated copper grid (400 mesh), respectively, after drying in vacuum.

Protein Sensing Experiments. The stock solutions of the required proteins were prepared by dissolving in 25 mM sodium dihydrogen phosphate and 10 mM sodium chloride. Concentrations of these stock solutions were calculated from the absorbance at a particular wavelength and molar extinction coefficient values. 0−100 μL of protein from the stock solution (4.2×10^{-4} M, phosphate buffer at pH 8.0) was added to a stirring solution of **Sq** nanoparticles (6×10^{-6} M, phosphate buffer at pH 8.0) in a glass cuvette with a path length of 1 cm at room temperature (25 °C). The solution was kept for 15 min, and the fluorescence intensity at 480 nm was measured after exciting at 380 nm. For protein selectivity studies, 100 μL of different proteins and small molecules from the stock solution (4.2×10^{-3} M, phosphate buffer at pH 8.0) were added slowly to a stirring solution of **Sq** nanoparticles (6×10^{-6} M) and kept for 1 h at room temperature. The change of fluorescence intensity at 480 nm was measured at an excitation wavelength of 380 nm.

Estimation of HSA in Human Blood Serum. Blood samples (3 mL each) were collected from healthy donors into a blood collecting tube using sterilized syringe and needle. The blood samples were allowed to clot by leaving it undisturbed at room temperature for 15−30 min. The blood samples were centrifuged (Biofuge stratus, Heracus instrument, Germany) at 3000 rpm for 10 min at 4 °C to separate the serum from the red blood cells. Serum on the top portion is then pipetted out into another vial which was used for the analysis. The HSA content in blood serum was estimated with **Sq** nanoparticles by using standard addition method. A calibration plot was prepared by measuring the emission maximum at 480 nm (I_{480}) upon addition of different concentration of HSA (3×10^{-7} to 9×10^{-7} M) to the **Sq** nanoparticles (6×10^{-6} M). The unknown concentration of HSA protein in the blood serum was calculated from the calibration curve by diluting the serum sample appropriately within the linear range.

Interaction of Sq Nanoparticles with Reduced Proteins. Protein (4×10^{-4} M) and DTT (4×10^{-2} M) solutions dissolved in phosphate buffer at pH 8.0 were taken in a 2 mL round-bottom flask and was refluxed in a water bath for 4 h. After cooling, the solutions were syringed out into a dialysis membrane of pore size 1000 and kept for dialysis for 24 h in a 1 L beaker filled with phosphate buffer having pH 8.0. The buffer solution was replaced each 2 h interval to remove the excess DTT and its oxidized products. Presence of more numbers of sulfhydryl groups in the reduced proteins were confirmed using DTNB (5,5′-dithio-bis-(2-nitrobenzoic acid)) reagent.[31] The denatured protein (4×10^{-4} M) from the dialysis membrane (45 μL) was added to **Sq** nanoparticles (6×10^{-6} M), prepared in 3 mL phosphate buffer at pH 8.0, and the emission intensity at 480 nm was recorded after keeping for 1 h.

■ ASSOCIATED CONTENT

Supporting Information

Materials, instruments, synthesis, and characterization of compounds, experimental procedures, and supplementary figures and schemes. This material is available free of charge via the Internet at http://pubs.acs.org.

■ AUTHOR INFORMATION

Corresponding Author

ajayaghosh@niist.res.in

Notes

The authors declare no competing financial interest.

■ ACKNOWLEDGMENTS

We thank CSIR, Government of India, New Delhi for financial support under NWP-023, DST and Dept. Atomic Energy, Government of India for a DAE-SRC Outstanding Researcher Award to A.A. P.A. and S.S. are grateful to CSIR for fellowships.

■ REFERENCES

(1) (a) Lehn, J.-M. *Supramolecular Chemistry: Concepts and Perspectives*; VCH: Weinheim, Germany, 1995. (b) *Molecular Self-Assembly: Advances and Applications*; Dequan, A. L., Ed.; Pan Stanford Publishing Pte Ltd.: Singapore, 2012. (c) Whitesides, G. M.; Grzybowski, B. *Science* **2002**, *295*, 2418. (d) Kinbara, K.; Aida, T. *Chem. Rev.* **2005**, *105*, 1377. (e) Ajayaghosh, A.; Praveen, V. K. *Acc. Chem. Res.* **2007**, *40*, 644. (f) Aida, T.; Meijer, E. W.; Stupp, S. I. *Science* **2012**, *335*, 813. (g) Busseron, E.; Ruff, Y.; Moulin, E.; Giuseppone, N. *Nanoscale* **2013**, *5*, 7098. (h) Babu, S. S.; Praveen, V. K.; Ajayaghosh, A. *Chem. Rev.* **2014**, *114*, 1973. (i) Zhang, S. *Nat. Biotechnol.* **2007**, *2*, 318. (j) Boekhoven, J.; Stupp, S. I. *Adv. Mater.* **2014**, *26*, 1642. (k) Zhai, D.; Xu, W.; Zhang, L.; Chang, Y. T. *Chem. Soc. Rev.* **2014**, *43*, 2402.

(2) Kartha, K. K.; Babu, S. S.; Srinivasan, S.; Ajayaghosh, A. *J. Am. Chem. Soc.* **2012**, *134*, 4834.

(3) (a) Kobayashi, H.; Ogawa, M.; Alford, R.; Choyke, P. L.; Urano, Y. *Chem. Rev.* **2010**, *110*, 2620. (b) Noble, J.; Porter, R.; Horgan, A. *Chem. Soc. Rev.* **2011**, *40*, 1547. (b) Chan, J.; Dodani, S. C.; Chang, C. J. *Nat. Chem.* **2012**, *4*, 973. (d) Vendrell, M.; Zhai, D.; Er, J. C.; Chang, Y. T. *Chem. Rev.* **2012**, *112*, 4391. (e) Saha, K.; Agasti, S. S.; Kim, C.; Li, X.; Rotello, V. M. *Chem. Rev.* **2012**, *112*, 2739. (f) Mizakami, S.; Hori, Y.; Kikuchi, K. *Acc. Chem. Res.* **2014**, *47*, 247.

(4) (a) Oh, K. J.; Cash, K. J.; Plaxco, K. W. *J. Am. Chem. Soc.* **2006**, *128*, 14018. (b) Thurley, S.; Roglin, L.; Seitz, O. *J. Am. Chem. Soc.* **2007**, *129*, 12693.

(5) (a) Wang, B.; Yu, C. *Angew. Chem., Int. Ed.* **2010**, *49*, 1485. (b) Tang, D.; Liao, D.; Zhu, Q.; Wang, F.; Jiao, H.; Zhang, Y.; Yu, C. *Chem. Commun.* **2011**, *47*, 5485. (c) Shi, H.; He, X. X.; Wang, K. M.; Wu, X.; Ye, X. S.; Guo, Q. P.; Tan, W. H.; Qing, Z. H.; Yang, X. H.; Zhou, B. *Proc. Natl. Acad. Sci. U.S.A.* **2011**, *108*, 3900.

(6) Sakabe, M.; Asanuma, D.; Kamiya, M.; Iwatate, R. J.; Hanaoka, K.; Terai, T.; Nagano, T.; Urano, Y. *J. Am. Chem. Soc.* **2013**, *135*, 409.

(7) (a) Xing, B.; Khanamiryan, A.; Rao, J. H. *J. Am. Chem. Soc.* **2005**, *127*, 4158. (b) Shults, M. D.; Imperiali, B. *J. Am. Chem. Soc.* **2003**, *125*, 14248. (c) Zhuang, Y. D.; Chiang, P. Y.; Wang, C. W.; Tan, K. T. *Angew. Chem., Int. Ed.* **2007**, *46*, 4097.

(8) (a) Suzuki, Y.; Yokoyama, K. *J. Am. Chem. Soc.* **2005**, *127*, 17799. (b) Yuan, C. X.; Tao, X. T.; Wang, L.; Yang, J. X.; Jiang, M. H. *J. Phys. Chem. C* **2009**, *113*, 6809. (c) Ojha, B.; Das, G. *Chem. Commun.* **2010**, *46*, 2079. (d) Wang, X.; Wang, X.; Wang, Y.; Guo, Z. *Chem. Commun.* **2011**, *47*, 8127. (e) Wang, J.; Liu, H. B.; Park, S.; Kim, S. Y.; Joo, T.; Ha, C. S. *RSC Adv.* **2012**, *2*, 4242. (f) Li, H.; Liu, F.; Han, J.; Cai, M.; Sun, S.; Fan, J.; Songa, F.; Peng, X. *J. Mater. Chem. B* **2013**, *1*, 693. (g) Peng, L.; Wei, R.; Li, K.; Zhou, Z.; Song, P.; Tong, A. *Analyst* **2013**, *138*, 2068.

(9) (a) Azagarsamy, M. A.; Sokkalingam, P.; Thayumanavan, S. *J. Am. Chem. Soc.* **2009**, *131*, 14184. (b) Yesilyurt, V.; Ramireddy, R.; Azagarsamy, M. A.; Thayumanavan, S. *Chem.−Eur. J.* **2012**, *18*, 223.

(10) (a) Guo, J.; Zhuang, J.; Wang, F.; Raghupathi, K. R.; Thayumanavan, S. *J. Am. Chem. Soc.* **2014**, *136*, 2220. (b) Torres, D. A.; Garzoni, M.; Subrahmanyam, A. V.; Pavan, G. V.; Thayumanavan, S. *J. Am. Chem. Soc.* **2014**, *136*, 5385.

(11) (a) Takaoka, Y.; Sakamoto, T.; Tsukiji, S.; Narazaki, M.; Matsuda, T.; Tochio, H.; Shirakawa, M.; Hamachi, I. *Nat. Chem.* **2009**,

1, 557. (b) Tsukiji, S.; Miyagawa, M.; Takaoka, Y.; Tamura, T.; Hamachi, I. *Nat. Chem. Biol.* **2009**, *5*, 341. (c) Mizusawa, K.; Ishida, Y.; Takaoka, Y.; Miyagawa, M.; Tsukiji, S.; Hamachi, I. *J. Am. Chem. Soc.* **2010**, *132*, 7291.
(12) (a) Mizusawa, K.; Takaoka, Y.; Hamachi, I. *J. Am. Chem. Soc.* **2012**, *134*, 13386. (b) Takaoka, Y.; Ojida, A.; Hamachi, I. *Angew. Chem., Int. Ed.* **2013**, *52*, 4088. (c) Hayashi, T.; Hamachi, I. *Acc. Chem. Res.* **2012**, *45*, 1460.
(13) (a) Miranda, O. R.; You, C. C.; Phillips, R.; Kim, I. B.; Ghosh, P. S.; Bunz, U. H. F.; Rotello, V. M. *J. Am. Chem. Soc.* **2007**, *129*, 9856. (b) You, C. C.; Miranda, O. R.; Gider, B.; Ghosh, P. S.; Kim, I. B.; Erdogan, B.; Krovi, S. A.; Bunz, U. H. F.; Rotello, V. M. *Nat. Nanotechnol.* **2007**, *2*, 318. (c) De, M.; Rana, S.; Akpinar, H.; Miranda, O. R.; Arvizo, R. R.; Bunz, U. H. F.; Rotello, V. M. *Nat. Chem.* **2009**, *1*, 461. (d) Rana, S.; Singla, A. K.; Bajaj, A.; Elci, S. G.; Miranda, O. R.; Mout, R.; Yan, B.; Jirik, F. R.; Rotello, V. M. *ACS Nano* **2012**, *6*, 8233.
(14) (a) Zhang, Y. Z.; Zhou, B.; Zhang, X. P.; Huang, P.; Li, C. H.; Liu, Y. *J. Hazard. Mater.* **2009**, *163*, 1345. (b) Ding, F.; Li, N.; Han, B. Y.; Liu, F.; Zhang, L.; Sun, Y. *Dyes Pigm.* **2009**, *83*, 249.
(15) (a) Zhu, J.; Li, J. J.; Zhao, J. W. *Sens. Actuators, B* **2009**, *138*, 9. (b) Wang, J.; Zhang, Y. Y.; Guo, Y.; Zhang, L.; Xu, R.; Xing, Z. Q.; Wang, S. X.; Zhang, X. D. *Dyes Pigm.* **2009**, *80*, 271. (c) Wen, J. H.; Geng, Z. R.; Yin, Y. X.; Wang, Z. L. *Dalton Trans.* **2011**, *40*, 9737.
(16) (a) Chen, X.; Zhou, Y.; Peng, X.; Yoon, J. *Chem. Soc. Rev.* **2010**, *39*, 2120. (b) Zhou, Y.; Yoon, J. *Chem. Soc. Rev.* **2012**, *41*, 52. (c) Jung, H. S.; Chen, X.; Kim, J. S.; Yoon, J. *Chem. Soc. Rev.* **2013**, *42*, 6019.
(17) (a) Yin, C.; Huo, F.; Zhang, J.; Martínez-Mánāz, R.; Yang, Y.; Lv, H.; Li, S. *Chem. Soc. Rev.* **2013**, *42*, 6032. (b) Lee, M. H.; Yang, Z.; Lim, C. W.; Lee, Y. H.; Sun, D.; Kang, C.; Kim, J. S. *Chem. Rev.* **2013**, *113*, 5071. (c) Yang, Y.; Zhao, Q.; Feng, W.; Li, F. *Chem. Rev.* **2013**, *113*, 192.
(18) (a) Ajayaghosh, A. *Acc. Chem. Res.* **2005**, *38*, 449. (b) Sreejith, S.; Carol, P.; Chithra, P.; Ajayaghosh, A. *J. Mater. Chem.* **2008**, *18*, 264. (c) Beverina, L.; Salice, P. *Eur. J. Org. Chem.* **2010**, 1207.
(19) (a) Gassensmith, J. J.; Arunkumar, E.; Barr, L.; Baumes, J. M.; DiVittorio, K. M.; Johnson, J. R.; Noll, B. C.; Smith, B. D. *J. Am. Chem. Soc.* **2007**, *129*, 15054. (b) Ajayaghosh, A.; Arunkumar, E.; Daub, J. *Angew. Chem., Int. Ed.* **2002**, *41*, 1766. (c) Basheer, M. C.; Alex, S.; Thomas, K. G.; Suresh, C. H.; Das, S. *Tetrahedron* **2006**, *62*, 605. (d) Ros-Lis, J. V.; Martinez-Manez, R.; Rurack, K.; Sancenon, F.; Soto, J.; Spieles, M. *Inorg. Chem.* **2004**, *43*, 5183. (e) Gassensmith, J. J.; Matthys, S.; Lee, J. J.; Wojcik, A.; Kamat, P. V.; Smith, B. D. *Chem.—Eur. J.* **2010**, *16*, 2916.
(20) (a) Ros-Lis, J. V.; Garcia, B.; Jimenez, D.; Martinez-Manez, R.; Sancenon, F.; Soto, J.; Gonzalvo, F.; Valldecabres, M. C. *J. Am. Chem. Soc.* **2004**, *126*, 4064. (b) Hewage, H. S.; Anslyn, E. V. *J. Am. Chem. Soc.* **2009**, *131*, 13099. (c) Sreejith, S.; Divya, K. P.; Ajayaghosh, A. *Angew. Chem., Int. Ed.* **2008**, *47*, 7883.
(21) (a) Suzuki, Y.; Yokoyama, K. *Angew. Chem., Int. Ed.* **2007**, *46*, 4097. (b) Jisha, V. S.; Arun, K. T.; Hariharan, M.; Ramaiah, D. *J. Am. Chem. Soc.* **2006**, *128*, 6024. (c) Jisha, V. S.; Arun, K. T.; Hariharan, M.; Ramaiah, D. *J. Phys. Chem. B* **2010**, *114*, 5912. (d) Xu, Y. Q.; Li, Z. Y.; Malkovskiy, A.; Sun, S. G.; Pang, Y. *J. Phys. Chem. B* **2010**, *114*, 8574.
(22) (a) Escobedo, J. O.; Rusin, O.; Lim, S.; Strongin, R. M. *Curr. Opin. Chem. Biol.* **2010**, *14*, 64. (b) Sreejith, S.; Ma, X.; Zhao, Y. L. *J. Am. Chem. Soc.* **2012**, *134*, 17346. (c) Baumes, J. M.; Gassensmith, J. J.; Giblin, J.; Lee, J. J.; White, A. G.; Culligan, W. J.; Leevy, W. M.; Kuno, M.; Smith, B. D. *Nat. Chem.* **2010**, *2*, 1025.
(23) (a) Zhang, Y.; Yue, X.; Kim, B.; Yao, S.; Bondar, M. V.; Belfield, K. D. *ACS Appl. Mater. Interfaces* **2013**, *5*, 8710. (b) Ahn, H. Y.; Yao, S.; Wang, X.; Belfield, K. D. *ACS Appl. Mater. Interfaces* **2012**, *4*, 2847.
(24) Gao, F.-P.; Lin, Y.-X.; Li, L.-L.; Liu, Y.; Mayerhöffer, U.; Spenst, P.; Su, J.-G.; Li, J.-Y.; Würthner, F.; Wang, H. *Biomaterials* **2014**, *35*, 1004.
(25) (a) Chen, H. J.; Law, K. Y.; Perlstein, J.; Whitten, D. G. *J. Am. Chem. Soc.* **1995**, *117*, 7257. (b) Arunkumar, E.; Forbes, C. C.; Noll, B. C.; Smith, B. D. *J. Am. Chem. Soc.* **2005**, *127*, 3288.
(26) Azagarsamy, M. A.; Yesilyurt, V.; Thayumanavan, S. *J. Am. Chem. Soc.* **2010**, *132*, 4550.
(27) Albumin is generally measured by a dye-binding technique that utilizes the ability of albumin to form a stable complex with bromocresol green dye. This complex absorbs at a different wavelength than the unbound dye. This method may over estimate albumin by binding to other proteins (http://www.ncbi.nlm.nih.gov/books/NBK204) as well. Therefore the clinical analysis is a rough estimation of albumin, whereas our method is accurate to the third decimal.
(28) (a) Carter, D. C.; He, X. M. *Science* **1990**, *249*, 302. (b) He, X. M.; Carter, D. C. *Nature* **1992**, *358*, 209.
(29) (a) Keil, D.; Hartmann, H. *Dyes Pigm.* **2001**, *49*, 161. (b) Selms, R. C. D.; Fox, C. J.; Riodan, R. C. *Tetrahedron Lett.* **1970**, *11*, 781.
(30) (a) Eldo, J.; Arunkumar, E.; Ajayaghosh, A. *Tetrahedron Lett.* **2000**, *41*, 6241. (b) Eldo, J.; Ajayaghosh, A. *Org. Lett.* **2001**, *3*, 2595.
(31) Sedkak, J.; Lindasay, R. H. *Anal. Biochem.* **1968**, *25*, 192.